energies

Article

A Coherency Identification Method of Active Frequency Response Control Based on Support Vector Clustering for Bulk Power System

Cuicui Jin [1], Weidong Li [1,*], Liu Liu [1], Ping Li [2] and Xian Wu [1]

[1] School of Electrical Engineering, Dalian University of Technology, Dalian 116024, China
[2] State Grid Liaoning Electric Power Supply Co., Ltd., Electric Power Research Institute, Shenyang 110006, China
* Correspondence: wdli@dlut.edu.cn; Tel.: +86-139-4269-8900

Received: 11 June 2019; Accepted: 13 August 2019; Published: 16 August 2019

Abstract: Active frequency response (AFR) control is needed in current power systems. To solve the over-frequency problems of generators connected to non-disturbed buses during the AFR control period, the generators should be clustered into coherent groups. Thus, the control efficiency can be improved on the premise of ensuring control accuracy. Since the influencing factors (such as the model parameters, operation modes, and disturbance locations, etc.) of power system operation can be comprehensively reflected by the generator frequency, which is easily collected and calculated, the generator frequency can be used as the coherency identification input. In this paper, we propose a coherency identification method of AFR control based on support vector clustering for a bulk power system. By mapping data samples from the initial space to the high-dimensional feature space, the radius of the minimal enclosing sphere that can envelop all the data samples is obtained. Moreover, the coherency identification of generators is determined for AFR control according to the evaluating method of AFR clustering control effects and the evaluating index of cluster compactness and separation. The simulation results for the modified New England IEEE 10-generator 39-bus system and Henan power grid show that the proposed method is feasible and effective.

Keywords: active frequency response; bulk power system; support vector clustering; wide area measurement system; frequency dynamic curve; primary frequency control

1. Introduction

With the gradual development of the ultra-high voltage (UHV) alternating current and direct current (DC) hybrid power grid and the significant increase of renewable energy penetration levels [1–3], the problem of active power imbalance after disturbance is increasingly prominent in power systems. The situation of frequency stability control becomes more severe [4,5]. Thus, the frequency security of power system cannot be ensured only with the traditional frequency response (primary frequency) control after large disturbance, and the active frequency response (AFR) control is needed [6,7].

The AFR control, which includes off-line analysis and on-line application, is different from the traditional frequency response control. It belongs to the centralized feed-forward control, which is regulated according to the pre-determined parameters. In off-line analysis, the typical scenarios should be formed by clustering the scenarios of existing operating states and the control decision table (including the following contents: the coherency identification of generators, the grading of the emergency levels, the selection of the control modes and parameters, and the dispatch of corrective actions, etc.) of each typical scenario should be completed. Thus, in on-line application, the current operation state can be matched to the typical scenario, and the corresponding control decision table can be used in real time and corrected on-line. The calculation process of AFR control is rather complex, and its on-line implementation is very difficult.

During the AFR control period, it is easy for over-frequency problems to occur on the generators connected to the non-disturbed buses. The formulation of the AFR control strategies is related to the control target, local frequency deviation, and regulation characteristic, etc., of each generator in a power system. If the control strategy and control decision table, etc., are formulated for each generator separately in the AFR control, the computation workloads are too heavy to be completed in off-line analysis, and the control commands are too many to be sent out quickly in on-line application. Thus, to reduce the computation effort and improve the control efficiency on the premise of ensuring the control accuracy, the coherency identification of generators is needed in the AFR control.

The AFR control is event-driven, and its starting speed after disturbance is as quick as that of relay protection. Since the AFR control scenarios are relatively certain, including the serious N-1 contingencies (the DC blocking events of UHV transmission lines, the sudden out of service of large-capacity thermal and nuclear power units, etc.) and the cascading outages (N-k contingency scenario: for $k = 2$, 3 or more), etc., the coherent groups of generators can be identified in off-line analysis for various possible contingency scenarios of AFR control. The clustering results under different contingency scenarios (including different disturbance locations, different disturbance types, etc.,) are different. The coherency identification of generators for AFR control is affected by multiple influencing factors (such as the disturbance locations, disturbance types, operation modes, model parameters, etc.) of each power system, and the dimensions of these influencing factors are different. Thus, the influencing factors are difficult to be analyzed comprehensively. Considering that the frequency is the comprehensive result of the above influencing factors and it is easy to be collected and calculated, the frequency is used as the clustering basis for the coherency identification of generators in AFR control.

At present, the research studies on the coherency identification of generators have used several methods, such as the slow coherency method, the electromechanical distance measure method, and the relation factor method, etc. In [8], the slow coherency method is proposed according to the principle of singular perturbation, and thus, the coherency groups of generators are obtained by using the linearized power system model. The results indicate that the slow coherency-based grouping is almost insensitive to the locations and severity of the initial faults. In [9], a coherency identification approach based on the concept of electromechanical distance in the transient period is proposed. It can provide a logical basis for determining the model complexity of each coherent group of generators. In [10], the generators of the coherent groups are identified according to the defined relation factors, which can represent the relative coupling degree between the generators. These research studies are all based on the linearized power system models, and the grouping results of coherent generators are easily influenced by the model precision. Moreover, the influencing factors such as the operation modes and the fault types, etc., of each power system cannot be considered in the coherency identification of generators.

In the power system of China, the frequency collection and communication technologies have developed very maturely. All of the transformer substations of 500 kV and above voltage levels and most of the 220-kV ones are installed with phasor measurement units (PMU) [11,12], and the optical fibers in the power communication network have 100% coverage. The PMUs are capable of providing real-time measurements of a power system with a satellite-triggered time stamp in the intervals down to 20 ms [13]. Its characteristics (including high data sampling speed, and fast, real-time, and reliable data transmission, etc.) can meet the requirements of the on-line and synchronal high-density measurements. This provides a new way for the coherency identification of generators after disturbance. The existing methods based on the PMU measured data include the independent component analysis approach [14], the improved Laplacian eigenmap algorithm [15], the principal component analysis method [16], the graph theory method [17], the wavelet phase difference approach [18], and the dynamic coherency determination method [19], etc. These methods are all for the transient stability of a power system in which the clearance speed of faults is very fast (from milliseconds to seconds). Therefore, they cannot be applied in the AFR control directly, and the coherency identification method for the AFR control has not yet been involved.

The AFR control is the frequency stability control measure in the time scale from seconds to minutes after large disturbance. A coherency identification method of AFR control based on support vector clustering (SVC) for a bulk power system is proposed in this paper. The proposed method can be used to (1) solve the over-frequency problems of generators connected to the non-disturbed bus, (2) reduce the computation workloads of off-line analysis, and (3) improve the control efficiency of on-line application. Since the generator coherency can be reflected by the frequency dynamic curves of generators collected with PMUs, the data samples of each generator can be obtained from its frequency dynamic curve. By mapping the frequency data samples of each generator from the original space to the high-dimensional feature space, the minimal enclosing sphere can be calculated out with the sequential minimal optimization (SMO) algorithm [20]. Moreover, the radius of the minimal enclosing sphere can be adjusted with the width parameter of the Gaussian kernel function. With the proposed method, multiple clustering results of generators can be obtained, and the optimal clustering result can be determined according to the evaluating method of AFR clustering control effects and the evaluating index of cluster compactness and separation.

The proposed method is applied to the modified New England IEEE 10 generator 39-bus system and Henan power grid. The AFR control effects with clustering control are compared with those without clustering control in the two test systems. The study results demonstrate that the transient maximum frequency of generators can be reduced below the safe upper limit of system frequency; thus, the over-frequency problems of generators connected to the non-disturbed bus can be effectively solved.

This paper is organized as follows. In Section 2, the coherency identification input of AFR control is determined. In Section 3, the coherency identification method of AFR control based on SVC for a bulk power system is proposed, and the evaluating method of AFR clustering control effects is provided in Section 4. In Section 5, the simulation and analysis results are given and discussed. Finally, the conclusions are given in Section 6.

2. Coherency Identification Input of AFR Control

The major influencing factors (such as the model parameters, operation modes, and disturbance locations, etc.) of generator coherency can be reflected by the frequency/phase-angle dynamic curves collected with PMUs. After disturbance, the generators with similar frequency/phase-angle dynamic curves are referred to as coherent generators [21].

After disturbance, the dynamic process of frequency response can be roughly divided into two stages: the frequency decline stage and the frequency recovery stage. As shown in Figure 1, Δt_{AC} is the frequency decline stage, and Δt_{CB} is the frequency recovery stage. Under the AFR control, each generator needs to be regulated according to the control requirements of the disturbed bus in the dynamic process of frequency response [7]. In the frequency decline stage of the disturbed bus, the control targets of all the generators in a power system are to recover the frequency of the disturbed bus to the rated value. In the frequency recovery stage, owing to the successful prevention of the frequency decline, the control target of each generator is to recover its own frequency to the rated value.

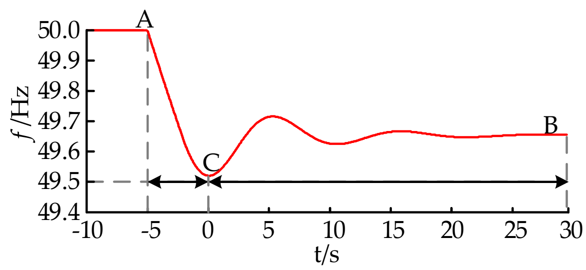

Figure 1. Dynamic process of frequency response.

During the AFR control period, when the generators connected to the non-disturbed bus provide power support for the disturbed bus, it is easier for the over-frequency problems to occur on the generators connected to the non-disturbed bus. The transient maximum frequency of some generators may be too high to implement the AFR control, and the frequency response capability of other generators has not been fully used. Considering that the generators with similar frequency dynamic curves can be managed and controlled uniformly in the frequency security constraint setting and the control strategy implementation, etc., the frequency can be used as the coherency identification input of AFR control. Thus, the frequency response capability of each generator can be fully used on the premise of ensuring the security of power system operation.

3. Coherency Identification of AFR Control Based on SVC for Bulk Power System

The SVC [22] is a non-parameter clustering algorithm based on support vector machine. The basic idea is to map the data samples from the initial space to the high-dimensional feature space with the Gaussian kernel function and obtain the minimal enclosing sphere that can envelop all the data samples in the high-dimensional feature space. New data samples can be accepted or rejected by the target cluster according to the contour of the minimal enclosing sphere. Among which, the data samples located outside of the minimal enclosing sphere are rejected by the target cluster, and the data samples located inside the minimal enclosing sphere are accepted. If the minimal enclosing sphere is mapped back to the original space, several closed curves in which some data samples are surrounded can be obtained. The data samples located in different closed curves belong to different clusters, and the similarity of the data samples in the same cluster is higher than that in different clusters.

The proposed method is essentially a dual convex quadratic programming problem. The purpose is to adjust the radius and contour of the minimal enclosing sphere by changing the width parameter of the Gaussian kernel function, and thus to obtain multiple clustering results of AFR control. Among which, the optimal clustering result can be obtained according to the evaluating method of AFR clustering control effects and the evaluating index of cluster compactness and separation.

3.1. Calculation of Minimal Enclosing Sphere

The AFR control is the frequency stability control measure in the time scale from seconds to minutes after large disturbance. The coherent generators can be identified with the PMU measured data of generator frequency in the initial period of frequency dynamic process. Among these, the frequency measurement of each generator bus (the bus that is connected to the generator) needs no steady-state test and is synchronous. To ensure the calculation accuracy, the highest sampling rates of PMU measured data are applied in the off-line calculation of the minimal enclosing sphere.

Take the generators as research objects and the PMU measured data as data samples. Then, compare the similarity among the data samples of generators. Among them, the data sample of generator i is:

$$\Delta \boldsymbol{f_i} = [\ldots\ \Delta f_i(t-\Delta t)\Delta f_i(t)\Delta f_i(t+\Delta t)\ \ldots]^T \tag{1}$$

where $\Delta \boldsymbol{f_i}$ is the frequency deviation vector, $t - \Delta t$, t, and $t + \Delta t$ are the sampling instants, and Δt is the sampling period.

The collection of the data samples of all the generators in a power system is:

$$\chi = \left\{\Delta \boldsymbol{f}_1, \Delta \boldsymbol{f}_2, \ldots, \Delta \boldsymbol{f_i}, \ldots, \Delta \boldsymbol{f}_N\right\}\ i \in \left[1, N\right] \tag{2}$$

where N is the number of generators, and $\Delta \boldsymbol{f_i} \in \mathbf{R}^d$.

By using the non-linear mapping $\boldsymbol{\Phi}$: $\mathbf{R}^d \to \mathbf{H}$, the data sample $\Delta \boldsymbol{f_i}$ of the generator i is mapped to the high-dimensional feature space $\mathbf{H}$, and the data sample $\boldsymbol{\Phi}(\Delta \boldsymbol{f_i})$ is obtained in the high-dimensional feature space $\mathbf{H}$. Assume that the radius of the minimal enclosing sphere enveloping all the data samples $\boldsymbol{\Phi}(\Delta \boldsymbol{f_i})$ in the high-dimensional feature space **H** is R, and thus, the solution of the radius of the minimal enclosing sphere satisfies:

$$\begin{cases} \min R^2 + C\sum\limits_{i=1}^{N} \xi_i \\ \| \boldsymbol{\Phi}(\Delta \boldsymbol{f_i}) - \boldsymbol{a} \|^2 \leq R^2 + \xi_i \;\; \forall i \end{cases} \tag{3}$$

where $\|\cdot\|$ is the Euclidean norm, $\boldsymbol{a}$ is the center of the enclosing sphere, C is the penalty factor, and ξ_i ($\xi_i \geq 0$) is the slack variable.

The corresponding Lagrangian function of Equation (3) is:

$$L(R, \boldsymbol{a}, \xi_i, \mu_i, \beta_i) = \min R^2 + C\sum_{i=1}^{N} \xi_i - \sum_{i=1}^{N} \xi_i \mu_i - \sum_{i=1}^{N} (R^2 + \xi_i - \| \boldsymbol{\Phi}(\Delta \boldsymbol{f_i}) - \boldsymbol{a} \|^2)\beta_i \tag{4}$$

where μ_i and β_i are the Lagrangian multipliers and $\mu_i \geq 0$, $\beta_i \geq 0$. Thus, the partial derivatives of Equation (4) with respect to R, $\boldsymbol{a}$, ξ_i are:

$$\sum_{i=1}^{N} \beta_i = 1 \tag{5}$$

$$\boldsymbol{a} = \sum_{i=1}^{N} \boldsymbol{\Phi}(\Delta \boldsymbol{f_i}) \tag{6}$$

$$\beta_i = C - \mu_i \tag{7}$$

The equations obtained based on the Karush-Kuhn-Tucker (KKT) conditions of Equation (4) satisfy:

$$\xi_i \mu_i = 0 \tag{8}$$

$$(R^2 + \xi_i - \| \boldsymbol{\Phi}(\Delta \boldsymbol{f_i}) - \boldsymbol{a} \|^2)\beta_i = 0 \tag{9}$$

It is known from Equations (8) and (9) that:

$$\beta_i = C \;\&\; \xi_i > 0 \;\Leftrightarrow\; R^2 < \| \boldsymbol{\Phi}(\Delta \boldsymbol{f_i}) - \boldsymbol{a} \|^2 \tag{10}$$

$$0 < \beta_i < C \;\&\; \xi_i = 0 \;\Leftrightarrow\; R^2 = \| \boldsymbol{\Phi}(\Delta \boldsymbol{f_i}) - \boldsymbol{a} \|^2 \tag{11}$$

$$\beta_i = 0 \;\&\; \xi_i = 0 \;\Leftrightarrow\; R^2 > \| \boldsymbol{\Phi}(\Delta \boldsymbol{f_i}) - \boldsymbol{a} \|^2 \tag{12}$$

that is, when $\beta_i = C$ and $\xi_i > 0$, the data sample $\boldsymbol{\Phi}(\Delta \boldsymbol{f_i})$ is located outside of the enclosing sphere. When $0 < \beta_i < C$ and $\xi_i = 0$, the data sample $\boldsymbol{\Phi}(\Delta \boldsymbol{f_i})$ is located on the surface of the enclosing sphere, and such a point is referred to as a support vector (SV). When $\beta_i = 0$ and $\xi_i = 0$, the data sample $\boldsymbol{\Phi}(\Delta \boldsymbol{f_i})$ is located inside the enclosing sphere.

Substituting Equations (5)–(9) into Equation (4), the dual function of the Lagrangian function (4) can be obtained:

$$\begin{cases} W = \max \sum\limits_{i=1}^{N} \boldsymbol{\Phi}(\Delta \boldsymbol{f_i})^2 \beta_i - \sum\limits_{i,j=1}^{N} \beta_i \beta_j \boldsymbol{\Phi}(\Delta \boldsymbol{f_i}) \cdot \boldsymbol{\Phi}(\Delta \boldsymbol{f_j}) \\ \text{subject to } 0 \leq \beta_i \leq C, \;\; i \in [1, N] \end{cases} \tag{13}$$

Define the Gaussian kernel function as:

$$K(\Delta \boldsymbol{f_i}, \Delta \boldsymbol{f_j}) = \boldsymbol{\Phi}(\Delta \boldsymbol{f_i}) \cdot \boldsymbol{\Phi}(\Delta \boldsymbol{f_j}) = e^{-q\|\Delta f_i - \Delta f_j\|^2} \tag{14}$$

where q is the width parameter. Thus, Equation (13) can be written as:

$$\begin{cases} W = \max \sum_{i=1}^{N} \beta_i K(\Delta \boldsymbol{f_i}, \Delta \boldsymbol{f_j}) - \sum_{i,j=1}^{N} \beta_i \beta_j K(\Delta \boldsymbol{f_i}, \Delta \boldsymbol{f_j}) \\ \text{subject to } 0 \le \beta_i \le C, \quad i \in [1, N] \end{cases} \tag{15}$$

Equation (15) is a quadratic programming optimization problem with respect to the variable β_i. The optimization process can be decomposed into the smallest possible scales in which only two data samples are optimized in each step with the SMO algorithm. When all the data samples are traversed and the KKT condition can be satisfied by all the variables β_i, the optimization process is terminated. With the SMO algorithm, the complex iteration problems faced by the numerical solution of quadratic programming can be effectively avoided. Thus, the calculation efficiency can be improved, and the calculation cumulative error can be eliminated. Moreover, the calculation speed and calculation accuracy can be ensured.

In the high-dimensional feature space, the distance from any data sample $\boldsymbol{\Phi}(\Delta \boldsymbol{f_i})$ to the center of the enclosing sphere satisfies:

$$\begin{aligned} R^2(\Delta f_i) \quad &= \| \boldsymbol{\Phi}(\Delta \boldsymbol{f_i}) - \boldsymbol{a} \|^2 \\ &= \| \boldsymbol{\Phi}(\Delta \boldsymbol{f_i}) - \sum_{j=1}^{\mathrm{N}} \boldsymbol{\Phi}(\Delta \boldsymbol{f_j}) \|^2 \\ &= K(\Delta \boldsymbol{f_i}, \Delta \boldsymbol{f_i}) - 2 \sum_{j=1}^{\mathrm{N}} \beta_j K(\Delta \boldsymbol{f_i}, \Delta \boldsymbol{f_j}) + \sum_{j,k=1}^{\mathrm{N}} \beta_j \beta_k K(\Delta \boldsymbol{f_j}, \Delta \boldsymbol{f_k}) \end{aligned} \tag{16}$$

Substituting the obtained variable β_i into Equation (16), the radius of the minimal enclosing sphere in which all the data samples $\boldsymbol{\Phi}(\Delta \boldsymbol{f_i})$ are enveloped can be obtained:

$$R = \{R(\boldsymbol{\Phi}(\Delta \boldsymbol{f_i})) | \boldsymbol{\Phi}(\Delta \boldsymbol{f_i}) \text{ is a SV.}\} \tag{17}$$

The contour of the minimal enclosing sphere satisfies:

$$\{x | R(x) = R\} \tag{18}$$

3.2. Allocation of Coherent Groups

Assume that the Generator i and j belong to two different coherent groups, and thus a point y, which is located outside of the minimal enclosing sphere obtained in Section 3.1, exists on the line segment connecting $\boldsymbol{\Phi}(\Delta \boldsymbol{f_i})$ and $\boldsymbol{\Phi}(\Delta \boldsymbol{f_j})$ in the high-dimensional feature space $\mathbf{H}$, satisfying $R(y) > R$. Define the adjacency matrix $\boldsymbol{A}$, which can express the adjacent relations among the generators in a power system as:

$$A_{i,j} = \begin{cases} 1 & \text{If all points on the segment connecting } \boldsymbol{\Phi}\left(\Delta \boldsymbol{f}_i\right) \text{ and } \boldsymbol{\Phi}\left(\Delta \boldsymbol{f}_j\right) \\ & \text{are located inside the enclosing sphere.} \\ 0 & \text{If a point } y \text{ on the segment connecting } \boldsymbol{\Phi}\left(\Delta \boldsymbol{f}_i\right) \text{ and } \boldsymbol{\Phi}\left(\Delta \boldsymbol{f}_j\right) \\ & \text{satisfies } R(y) > R. \end{cases} \tag{19}$$

Thus, the breadth-first search method [23] can be adopted to traverse all of the adjacent generator buses from a generator bus. Then, start from the above adjacent generator bus in turn, and access the remaining adjacent generator buses that have not been accessed, and so forth. When all of the generator buses are accessed, the search is completed, and the clustering result of generators is obtained.

The allocation of coherent groups in AFR control consists of off-line analysis and on-line application. In off-line analysis, the allocation of coherent groups should be completed for all possible contingency scenarios and each network configuration/dispatch situation. In on-line application, the current operation state should be on-line matched to the typical scenario, and the corresponding allocation method of coherent groups should be applied to the power system in real time. Among them, the allocation of coherent groups is event-triggered in the on-line application stage.

3.3. Selection of Clustering Results

The coherency identification of generators for AFR control is mainly considered from two aspects. From one aspect, the stronger the correlation among the generators in the same coherent group and the weaker the correlation among the generators in different coherent groups, the better the clustering result of generators [24]. From the other aspect, the smaller the number of the coherent groups of generators, the higher the control efficiency of the AFR control. Thus, the coherency of generators and the number of coherent groups should be balanced in the coherency identification of generators for the AFR control.

After disturbance, the correlation among the generators in the coherent group B_i satisfies:

$$d_{\text{intra}}(B_i) = \frac{1}{|SV_i|}\sum_{j=1}^{|SV_i|} \underset{\substack{\Delta f_k, \Delta f_j \in SV_i \\ 1 \le k \le |SV_i|}}{\operatorname{argmax}} \parallel \Delta \boldsymbol{f_j} - \Delta \boldsymbol{f_k} \parallel^2 \tag{20}$$

where $d_{\text{intra}}(B_i)$ denotes the intra-cluster distance, SV_i represents the collection of the SVs in coherent group B_i, and $|SV_i|$ is the corresponding number of SVs. The smaller the $d_{\text{intra}}(B_i)$, the stronger the correlation among the generators in the coherent group B_i.

The correlation between the generators in the coherent group B_i and the generators in the coherent group B_j satisfies:

$$d_{\text{inter}}(B_i) = \underset{\Delta f_l \in SV_i, \Delta f_k \in SV_j}{\operatorname{argmin}} \parallel \Delta \boldsymbol{f_l} - \Delta \boldsymbol{f_k} \parallel^2 \tag{21}$$

where $d_{\text{inter}}(B_i)$ denotes the inter-cluster distance between the generators in coherent group B_i and those in coherent group B_j. The larger the $d_{\text{inter}}(B_i)$, the weaker the correlation between the coherent groups B_i and B_j.

Define the evaluating index of cluster compactness and separation as:

$$V(m) = \frac{\sum_{i=1}^{m} d_{\text{intra}}(B_i)}{\sum_{i=1}^{m} d_{\text{inter}}(B_i)} \tag{22}$$

where m is the number of coherent groups. The smaller the $V(m)$, the better the clustering result.

In the high-dimensional feature space, with the increase of the width parameter of the Gaussian kernel function, the number of the coherent groups is increased. The optimal evaluating index of cluster compactness and separation satisfies:

$$V_o = \min_{q_{\min} \le q \le q_{\max}} V(m) \tag{23}$$

where:

$$q_{\min} = \frac{1}{\max_{1 \le i,j \le N, i \ne j} \parallel \Delta \boldsymbol{f_i} - \Delta \boldsymbol{f_j} \parallel^2} \tag{24}$$

$$q = q_{\min} + q_{\text{step}} \tag{25}$$

Among which, $q_{\min}$ is the minimal width parameter of the Gaussian kernel function, and q_{step} is the increment of the width parameter.

The coherency identification of generators for the AFR control includes off-line analysis and on-line application. For the same typical scenario, the AFR control effects of different clustering results should be compared in the increasing order of m in off-line analysis with the method in

Section 4. Among them, the smallest $V(m)$ should be selected from the clustering results with which the over-frequency problems can be effectively avoided. Thus, the optimal clustering result of AFR control can be obtained.

3.4. Calculation Process

The calculation process of the proposed coherency identification method of AFR control based on SVC for a bulk power system is shown in Figure 2. The specific calculation steps are as follows:

Step 1: Based on the PMU measured data of generator frequency, the data samples of generators are obtained and then input.
Step 2: The relevant parameters are initialized, among which $q = q_{\min}$.
Step 3: The data samples are mapped from the initial space to the high-dimensional feature space, and the radius and contour of the minimal enclosing sphere are obtained with the SMO algorithm.
Step 4: The clustering results of generators are obtained with the breadth-first search method.
Step 5: The evaluating indexes of cluster compactness and separation are calculated out.
Step 6: Let $q = q_{\min} + q_{\text{step}}$, and if the number of coherent groups is less than $N - 1$, repeat steps 3 to 5. Otherwise, jump out the SVC algorithm.
Step 7: The AFR clustering control effects and the evaluating indexes of cluster compactness and separation under different width parameters, q, are compared. Thus, the optimal clustering result of AFR control is obtained.

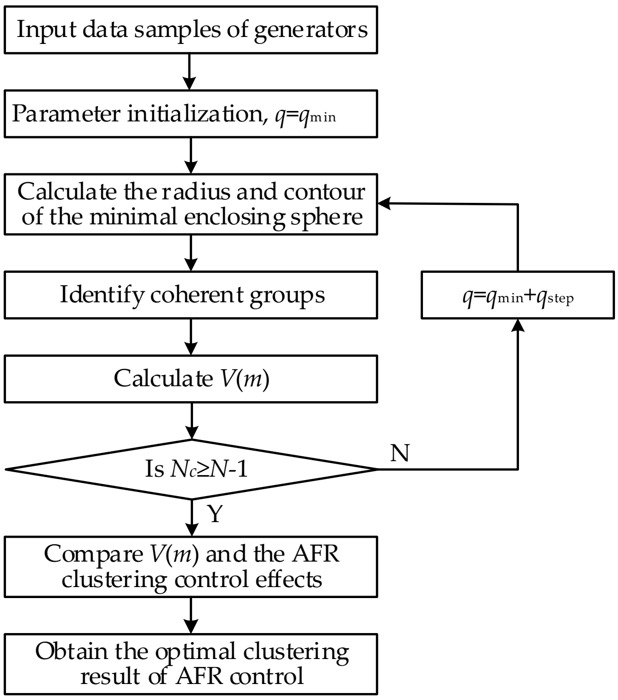

Figure 2. Calculation process of the proposed method.

4. Evaluation of AFR Clustering Control Effects

The AFR control is the centralized and feed-forward control that is regulated according to the parameters determined in off-line analysis. The parameters can be the frequency deviation signals of the disturbed bus, local bus, or other buses, etc. in the power system. At present, a preliminary AFR strategy [6] and an AFR strategy based on model predictive control (the MPC-AFR strategy) [7] have been proposed. Since the MPC-AFR strategy is very complex and further research is still needed in the practical application, the preliminary AFR strategy is selected in this paper.

It is assumed that the local frequency deviation of the disturbed bus is Δf_r, the time when the frequency of the disturbed bus reaches the frequency nadir is t_{nadir}, the control parameter of the disturbed bus is c_A, the local frequency deviation of the non-disturbed bus is Δf_l, and the control parameter of the non-disturbed bus is c_B.

Under the AFR control, if the clustering control is not adopted, the generators are regulated according to the pre-determined parameters (determined according to the maximum frequency deviation of the disturbed bus under traditional frequency response control) in the frequency decline stage, and the control mode is feed-forward control. In the frequency recovery stage, the generators are regulated according to the local frequency deviations, and the control mode is feedback control. Thus, the control parameters of the disturbed bus and the non-disturbed bus satisfy:

$$c_A = c_B = \begin{cases} \max\Delta f_r & 0 < t \le t_{nadir} \\ \Delta f_l & t > t_{nadir} \end{cases} \tag{26}$$

Although the frequency response capability of all the generators can be fully used and the frequency nadir of the disturbed bus can be raised to the utmost with the above control mode, the frequency of the generators connected to the non-disturbed bus is negatively affected. On the one hand, the over-frequency problems may occur on the generators connected to the non-disturbed bus during the AFR period. On the other hand, the frequency oscillation phenomenon of the generators connected to the non-disturbed bus becomes more obvious.

To solve the above problems, the AFR control strategy of each generator should be respectively formulated in principle. However, because the formulation of the AFR control strategy for each generator is not only complex but also meaningless, the clustering control is adopted in the AFR control. In the AFR clustering control, the generators are regulated according to the pre-determined parameters of the coherent group (determined according to the maximum frequency deviation of the generators in the coherent group under traditional frequency response control) in the frequency decline stage, and the control mode is feed-forward control. In the frequency recovery stage, the generators are regulated according to the local frequency deviations, and the control mode is feedback control. Thus, the control parameters of the disturbed bus and the non-disturbed bus satisfy:

$$c_A = c_B = \begin{cases} \max\Delta f_{lcluster} & 0 < t \le t_{nadir} \\ \Delta f_l & t > t_{nadir} \end{cases} \tag{27}$$

where $\Delta f_{lcluster}$ is the maximum frequency deviation of the generators in the coherent group under traditional frequency response control.

The research emphasis of AFR control is the frequency nadir (the purpose of the AFR control is to make the frequency nadir of the power system greater than the under-frequency load-shedding threshold after large disturbance) and the transient maximum frequency of power systems. Thus, if the over-frequency problems of power systems can be avoided on the premise of ensuring the AFR control effect on the frequency nadir with the clustering control, the clustering control should be adopted. Moreover, the clustering result with a fewer number of coherent groups should be given priority to improve the AFR control efficiency.

5. Case Studies

To validate the effectiveness of the proposed coherency identification method of AFR control based on SVC for a bulk power system, the modified New England IEEE 10-generator 39-bus system and Henan power grid are modeled and simulated with Matlab/Simulink. Among them, the generator models are from [7], and the connection relationships among generators are the same as the system topologies.

In the section, the modified New England IEEE 10-generator 39-bus system—which is not a bulk power system, but still has certain frequency time-space distribution characteristics—is used to present the calculation process of the proposed method. The Henan power grid, which is a provincial power system in China and has been used in the research of AFR control [7], is used to verify the effectiveness of the proposed method in a practical bulk power system.

It is assumed that the under-frequency load-shedding threshold, the safe upper limit of system frequency, and the rated frequency are 49.5 Hz, 50.2 Hz, and 50 Hz, respectively. The SVC parameters satisfy that the penalty factor is 1 and the slack variable is 0.2.

5.1. Modified New England IEEE 10-Generator 39-Bus System

The modified New England IEEE 10-generator 39-bus system includes 10 generators, 39 buses, and 34 transmission lines, and the system topology is shown in Figure 3. It is assumed that the bus 30 is disturbed at 2 s and the step load disturbance is 0.135 p.u. Thus, the frequency dynamic curves of all the generator buses in the modified New England IEEE 10-generator 39-bus system are shown in Figure 4.

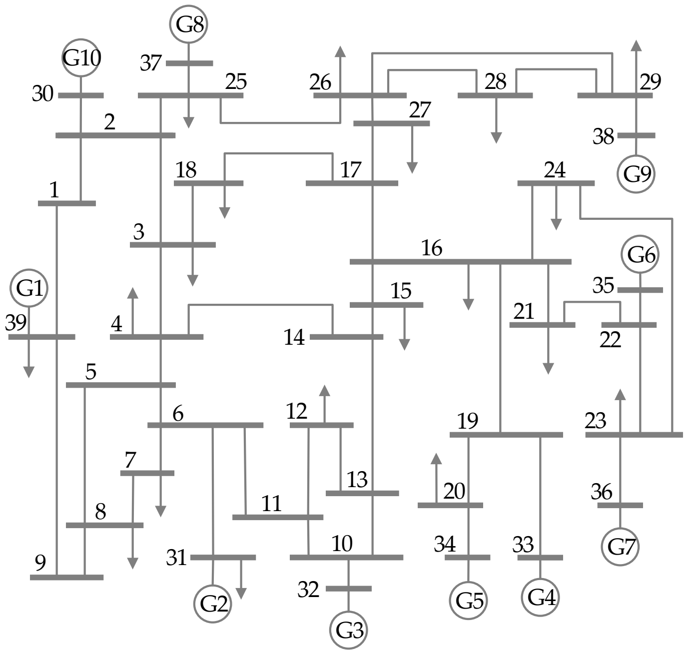

Figure 3. The topology of a modified New England IEEE 10-generator 39-bus system.

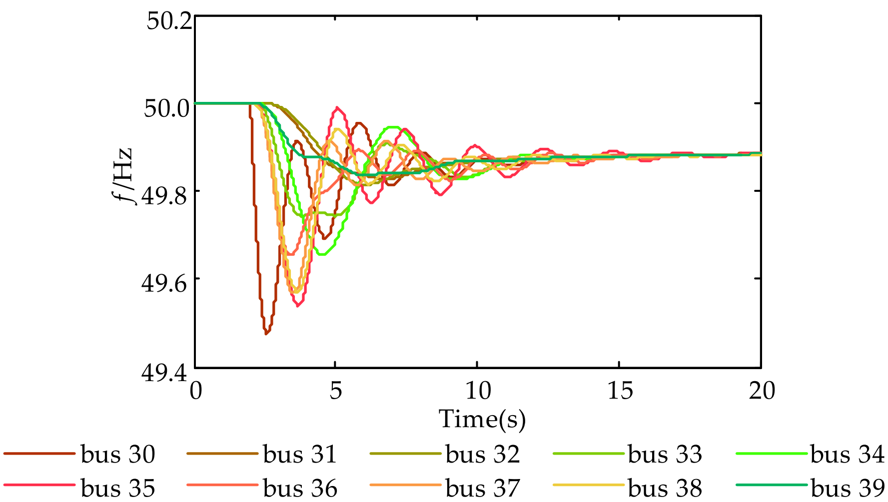

Figure 4. Frequency dynamic curves of the generator buses in a modified New England IEEE 10-generator 39-bus system.

As demonstrated in Figure 4, the frequency nadir of the modified New England IEEE 10-generator 39-bus system is 49.4825 Hz, and it is lower than the under-frequency load-shedding threshold. Thus, the AFR control is required. Since the differences among the frequency dynamic curves of generators are mainly reflected in the period from 2 s to 15 s, the data samples of generators can be obtained from the PMU measured data of the generator frequency in this period. With the SVC algorithm, seven clustering results of generators can be obtained, and these are shown in Table 1. Among them, when V_o = 0.1501, the optimal clustering result of generators for AFR control is obtained (as shown in Figure 5), and the number of the coherent groups is 3.

Table 1. Clustering results of generators after the disturbance of bus 30 in a modified New England IEEE 10-generator, 39-bus system.

Evaluating Index V_o	Number of Clusters m	Clustering Results of Generators
0.1501	3	{30}, {31,32,39}, {33,34,35,36,37,38}
0.1488	4	{30}, {31,32,39}, {33,34}, {35,36, 37,38}
0.1315	5	{30}, {31,32,39}, {33,34}, {35,37,38}, {36}
0.1235	6	{30}, {31,32,39}, {33,34}, {35,38}, {36}, {37}
0.0636	7	{30}, {31,32,39}, {33}, {34}, {35,38}, {36}, {37}
0.0207	8	{30}, {31,32,39}, {33}, {34}, {35}, {36}, {37}, {38}
0.0128	9	{30}, {31,32}, {33}, {34}, {35}, {36}, {37}, {38}, {39}

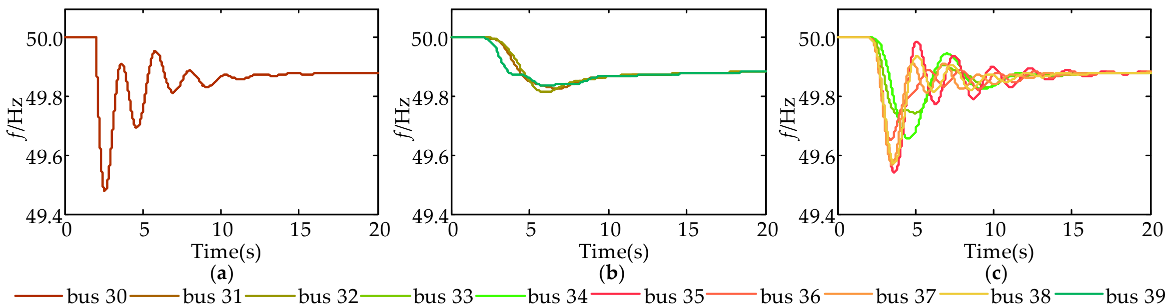

Figure 5. The optimal clustering result of generators after the disturbance of bus 30 in a modified New England IEEE 10-generator, 39-bus system. (**a**) Coherent group 1; (**b**) Coherent group 2; and (**c**) Coherent group 3.

When the number of the coherent groups of generators is three, the AFR control effects with and without the clustering control are shown in Figure 6. As shown in the simulation results, under the AFR control, if the clustering control is not adopted, the frequency nadir and the transient maximum frequency of the modified New England IEEE 10-generator 39-bus system are 49.5048 Hz and 50.2249 Hz, respectively. If the clustering control is adopted, the frequency nadir and the transient maximum frequency are 49.5046 Hz and 50.1866 Hz, respectively.

Known from comparative analysis, on the one hand, the frequency nadir is little affected by the AFR clustering control. Both the AFR clustering control and the AFR control without clustering control can make the frequency nadirs greater than the under-frequency load-shedding threshold (49.5 Hz). The AFR control effect on the frequency nadir can be ensured. On the other hand, the transient maximum frequency can be reduced by 0.0383 Hz with the AFR clustering control, and the decline is 17.03%. Compared with the AFR control without clustering control, the AFR clustering control can make the transient maximum frequency lower than the safe upper limit of system frequency (50.2 Hz). The over-frequency problems can be effectively avoided.

Thus, it can be seen that both the frequency nadir and the transient maximum frequency of the modified New England IEEE 10-generator 39-bus system can be controlled in the security constraint range of system frequency (in the range between 49.5–50.2 Hz) with the AFR clustering control.

The over-frequency problems can be effectively avoided on the premise of ensuring the security of the frequency nadir.

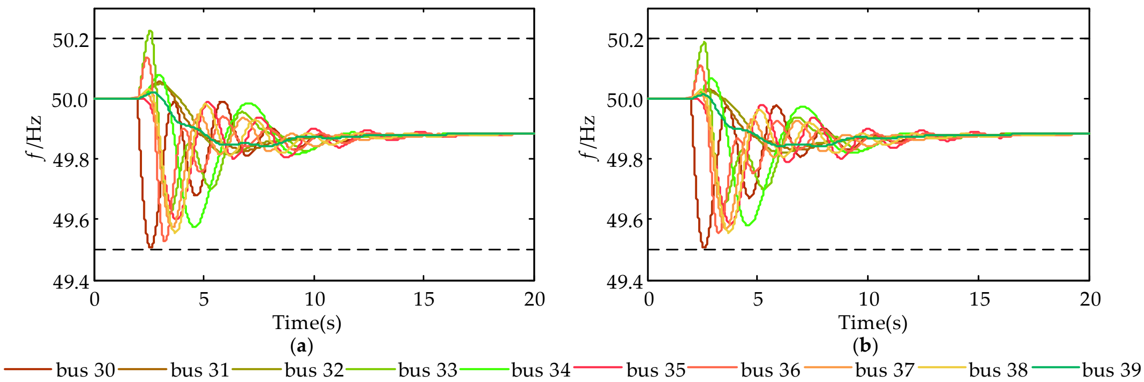

Figure 6. The active frequency response (AFR) control effects with and without the clustering control after the disturbance of bus 30 in a modified New England IEEE 10-generator 39-bus system. (**a**) The AFR control effect without the clustering control; (**b**) The AFR control effect with the clustering control.

5.2. Henan Power Grid

To further validate the effectiveness of the proposed method, all the generators in the Henan power grid are connected to the 500-kV grid structure according to the grid structures and generator locations of the Henan power grid. Moreover, the frequency dynamic curves of all the generators connected to the same generator bus are considered to be approximately similar.

In the Henan power grid, after the DC bipolar blocking fault of UHV transmission lines from Tianshan to Zhongzhou, the maximum power loss is 3.35 GW. It is assumed that the above UHV transmission lines are connected to bus 1, and the DC bipolar blocking fault happens at 2 s. If the power loss is at a maximum and the power support from other provincial power systems is ignored, the frequency dynamic curves of the generator buses on the 500-kV grid structure of the Henan power grid are shown in Figure 7.

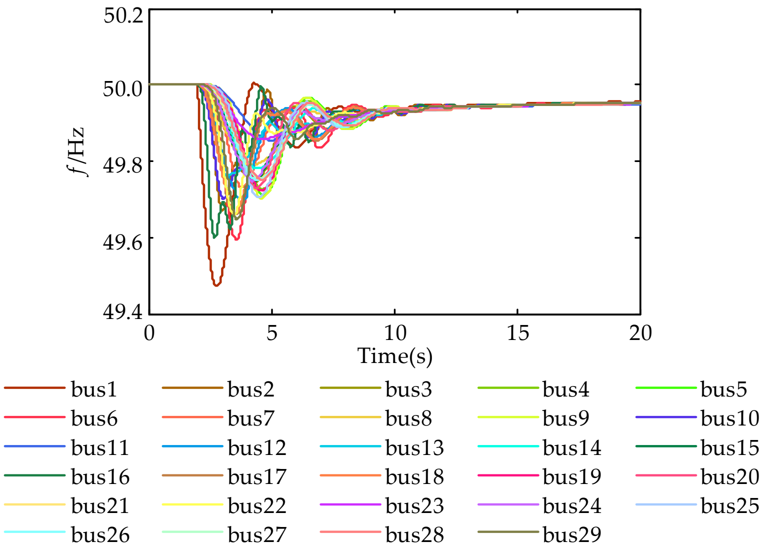

Figure 7. Frequency dynamic curves of the generator buses on the 500-kV grid structure of the Henan power grid.

As shown in Figure 7, the frequency nadir of the Henan power grid after disturbance is 49.4738 Hz, and the under-frequency load-shedding has been triggered. As in the above example, the multiple clustering results of the generator buses on the 500-kV grid structure of the Henan power grid can be obtained, and these are shown in Table 2. Among them, when V_o = 0.0650, the optimal clustering result can be obtained for the AFR control (as shown in Figure 8), and the number of the coherent groups is six.

Table 2. Clustering results of the generator buses on the 500-kV grid structure of the Henan power grid after the disturbance of bus 1.

Evaluating Index V_o	Number of Clusters m	Clustering Results of Generators
0.0814	2	{1}, {2, 3, 4, 5, 6, 7, 8, 9, 10, 11, 12, 13, 14, 15, 16, 17, 18, 19, 20, 21, 22, 23, 24, 25, 26, 27, 28, 29}
0.0767	4	{1}, {2, 3, 4, 5, 6, 7, 8, 9, 10, 12, 13, 14, 15, 17, 18, 19, 20, 21, 22, 24, 25, 26, 27, 28, 29}, {11, 23}, {16}
0.0708	5	{1}, {2, 6, 7, 10, 12, 13, 17, 18, 22, 29}, {3, 4, 5, 8, 9, 14, 15, 19, 20, 21, 24, 25, 26, 27, 28}, {11, 23}, {16}
0.0650	6	{1}, {2, 10}, {3, 4, 5, 8, 9, 14, 15, 19, 20, 21, 24, 25, 26, 27, 28}, {6, 7, 12, 13, 17, 18, 22, 29}, {11, 23}, {16}
0.0700	7	{1}, {2, 10}, {3, 4, 5, 8, 9, 14, 15, 19, 20, 21, 24, 25, 26, 27, 28}, {6, 7, 12, 17, 18, 22, 29}, {11, 23}, {13}, {16}
0.0652	9	{1}, {2, 10}, {3, 4, 5, 8, 9, 14, 15, 19, 20, 21, 24, 25, 26, 27, 28}, {6, 12, 17, 18, 29}, {7}, {11, 23}, {13}, {16}, {22}
0.0418	12	{1}, {2, 10}, {3, 4, 5, 8, 9, 14, 15, 19, 20, 21, 24, 25, 26, 27, 28}, {6}, {7}, {11, 23}, {12}, {13}, {16}, {17, 18}, {22}, {29}
0.0654	15	{1}, {2, 10}, {3, 20}, {4, 5, 9, 19, 21, 25, 26, 27, 28}, {6}, {7}, {8, 14}, {11, 23}, {12}, {13}, {15, 24}, {16}, {17, 18}, {22}, {29}
0.0674	17	{1}, {2, 10}, {3, 20}, {4, 5, 9, 19}, {6}, {7}, {8, 14}, {11, 23}, {12}, {13}, {15, 24}, {16}, {17, 18}, {21, 26, 27, 28}, {22}, {25}, {29}
0.0316	20	{1}, {2}, {3, 20}, {4, 5, 9, 19}, {6}, {7}, {8}, {10}, {11}, {12}, {13}, {14}, {15, 24}, {16}, {17, 18}, {21, 26, 27, 28}, {22}, {23}, {25}, {29}
0.0264	22	{1}, {2}, {3}, {4, 19}, {5, 9}, {6}, {7}, {8}, {10}, {11}, {12}, {13}, {14}, {15, 24}, {16}, {17, 18}, {20}, {21, 26, 27, 28}, {22}, {23}, {25}, {29}
0.0185	24	{1}, {2}, {3}, {4, 19}, {5, 9}, {6}, {7}, {8}, {10}, {11}, {12}, {13}, {14}, {15, 24}, {16}, {17}, {18}, {20}, {21, 27, 28}, {22}, {23}, {25}, {26}, {29}
0.0111	25	{1}, {2}, {3}, {4}, {5, 9}, {6}, {7}, {8}, {10}, {11}, {12}, {13}, {14}, {15, 24}, {16}, {17}, {18}, {19}, {20}, {21, 27, 28}, {22}, {23}, {25}, {26}, {29}
0.0051	27	{1}, {2}, {3}, {4}, {5}, {6}, {7}, {8}, {9}, {10}, {11}, {12}, {13}, {14}, {15, 24}, {16}, {17}, {18}, {19}, {20}, {21}, {22}, {23}, {25}, {26}, {27, 28}, {29}

When the number of the coherent groups of the generator buses on the 500-kV grid structure of the Henan power grid is six, the AFR control effects with and without the clustering control are shown in Figure 9. As demonstrated in the simulation results, under the AFR control, if the clustering control is not adopted, the frequency nadir and the transient maximum frequency of the Henan power grid are 49.5093 Hz and 50.2918 Hz, respectively. If the clustering control is adopted, the frequency nadir and the transient maximum frequency are 49.5162 Hz and 50.1931 Hz, respectively.

As in the above example, on the one hand, the frequency nadir is little affected by the AFR clustering control, and both AFR control strategies can make the frequency nadir of the Henan power grid greater than the under-frequency load-shedding threshold (50.2 Hz). Thus, the AFR control effect on the frequency nadir can be ensured. On the other hand, the transient maximum frequency of the Henan power grid can be reduced by 0.0987 Hz, and the decline is 33.82%. Compared with the AFR control without the clustering control, the AFR clustering control can make the transient maximum frequency lower than the safe upper limit of the system frequency (50.2 Hz). The over-frequency problems of the Henan power grid can be effectively avoided.

Thus, it can be seen that the over-frequency problems of the Henan power grid can be effectively avoided on the premise of ensuring the security of the frequency nadir. The proposed method is further verified in the Henan power grid.

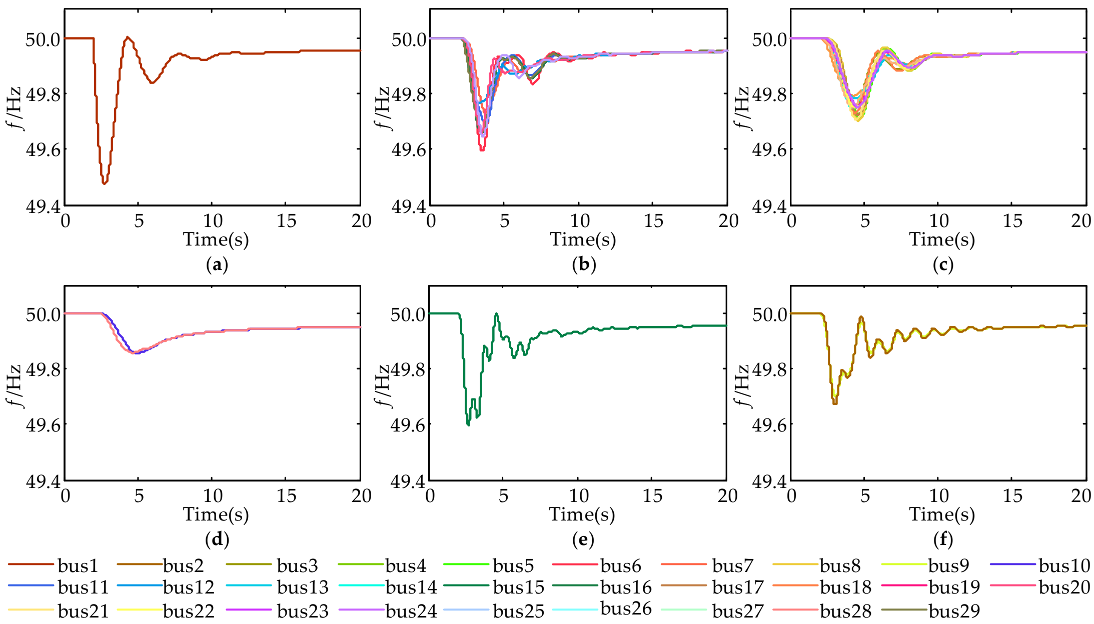

Figure 8. The optimal clustering result of the generator buses on the 500-kV grid structure of the Henan power grid after the disturbance of bus 1. (**a**) Coherent group 1; (**b**) Coherent group 2; (**c**) Coherent group 3; (**d**) Coherent group 4; (**e**) Coherent group 5; and (**f**) Coherent group 6.

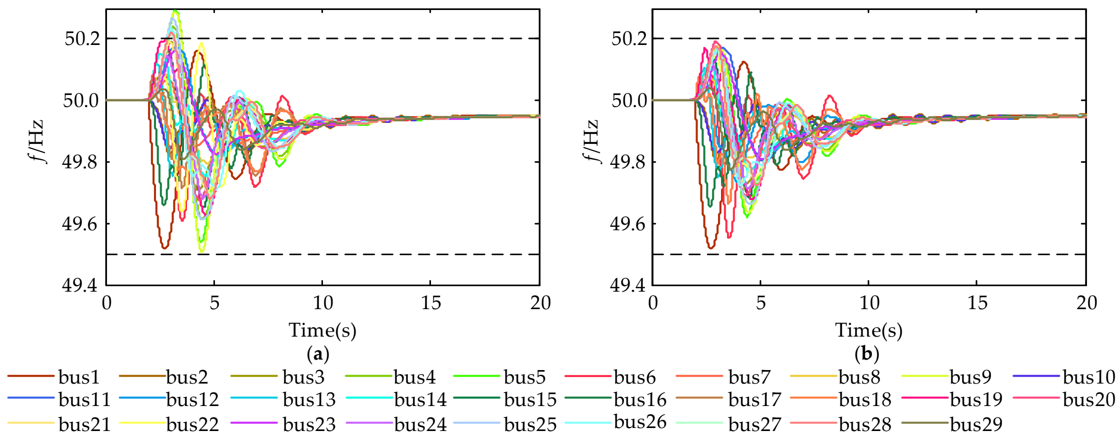

Figure 9. The AFR control effects with and without the clustering control after the disturbance of bus 1 in the Henan power grid. (**a**) The AFR control effect without the clustering control; (**b**) The AFR control effect with the clustering control.

6. Conclusions

To solve the over-frequency problems of the generators connected to the non-disturbed bus during the AFR control period, the coherency identification method of AFR control based on SVC for a bulk power system is proposed. The results of the theoretical research and simulation analysis can be drawn as follows.

(a) The generator frequency that can comprehensively reflect the effects of the disturbance location, operation modes, and model parameters, etc., of a power system on the clustering results can be used as the coherency identification input of AFR control. It has the characteristics of fewer parameters and smaller calculation. Thus, the input parameters are operational and convenient for practical application.

(b) The SVC algorithm is feasible and effective in the coherency identification of generators for AFR control, and it can provide multiple clustering results. On the premise of ensuring the control accuracy, the computation effort of off-line analysis can be reduced, and the control efficiency of on-line application can be improved.

(c) With the AFR clustering control, not only the frequency nadir of the power system is little affected, but the transient maximum frequency of the generators connected to the non-disturbed bus can also be reduced below the safe upper limit of system frequency. The over-frequency problems of AFR control can be effectively avoided on the premise of ensuring the security of the frequency nadir.

Author Contributions: C.J. and W.L. conceived and designed the research problem; C.J. wrote the whole manuscript; W.L. supervised the paper writing; L.L., P.L., and X.W. participated in results analysis.

Funding: This research was supported in part by National Natural Science Foundation of China, grant number 51677018.

Conflicts of Interest: The authors declare no conflict of interest.

References

1. Huang, D.; Shu, Y.; Ruan, J.; Hu, Y. Ultra High Voltage Transmission in China: Developments, Current Status and Future Prospects. *Proc. IEEE* **2009**, *97*, 555–583. [CrossRef]
2. Bi, T.; Qin, J.; Yan, Y.; Liu, H.; Martin, K.E. An Approach for Estimating Disturbance Arrival Time Based on Structural Frame Model. *IEEE Trans. Power Syst.* **2017**, *32*, 1741–1750. [CrossRef]
3. Dreidy, M.; Mokhlis, H.; Mekhilef, S. Inertia response and frequency control techniques for renewable energy sources: A review. *Renew. Sustain. Energy Rev.* **2017**, *69*, 144–155. [CrossRef]
4. Hatziargyriou, N.D.; Andersson, G.; Donalek, P.; Farmer, R.; Hatziargyriou, N.D.; Kamwa, I.; Kundur, P.; Martins, N.; Paserba, J.; Pourbeik, P. Causes of the 2003 Major Grid Blackouts in North America and Europe and Recommended Means to Improve System Dynamic Performance. *IEEE Trans. Power Syst.* **2005**, *20*, 1922–1928.
5. Egido, I.; Fernandez-Bernal, F.; Centeno, P.; Rouco, L. Maximum frequency deviation calculation in small isolated power systems. *IEEE Trans. Power Syst.* **2009**, *24*, 1731–1738. [CrossRef]
6. Li, W.; Jin, C.; Wen, K.; Shen, J.; Lin, L. Preliminary Research on active frequency response control under high power loss. *Autom. Electr. Power Syst.* **2018**, *42*, 22–30. (In Chinese)
7. Jin, C.; Li, W.; Shen, J.; Li, P.; Lin, L.; Wen, K. Active frequency response based on model predictive control for bulk power system. *IEEE Trans. Power Syst.* **2019**, *34*, 3002–3013. [CrossRef]
8. You, H.; Member, S.; Vittal, V.; Wang, X. Slow Coherency-Based Islanding. *IEEE Trans. Power Syst.* **2004**, *19*, 483–491. [CrossRef]
9. Pai, M.A.; Adgaonkar, R.P. Electromechanical distance measure for decomposition of power systems. *Int. J. Electr. Power Energy Syst.* **1984**, *6*, 249–254. [CrossRef]
10. Kim, H.; Jang, G.; Song, K. Dynamic reduction of the large-scale power systems using relation factor. *IEEE Trans. Power Syst.* **2004**, *19*, 1696–1699. [CrossRef]
11. Lu, B.C.; Shi, B.; Wu, X.; Sun, H. Advancing China's Smart Grid: Phasor measurement units in a wide-area management system. *IEEE Power Energy Mag.* **2015**, *13*, 60–71. [CrossRef]
12. Ma, J.; Zhang, P.; Fu, H.J.; Bo, B.; Dong, Z.Y. Application of phasor measurement unit on locating disturbance source for low-frequency oscillation. *IEEE Trans. Smart Grid* **2010**, *1*, 340–346. [CrossRef]
13. Zima, M.; Larsson, M.; Korba, P.; Rehtanz, C.; Andersson, G. Design Aspects for Wide-Area Monitoring and Control System. *Proc. IEEE* **2005**, *93*, 980–996. [CrossRef]
14. Ariff, M.A.M.; Pal, B.C. Coherency identification in interconnected power system–An independent component analysis approach. *IEEE Trans. Power Syst.* **2013**, *28*, 1747–1755. [CrossRef]
15. Song, H.; Wu, J.; Wu, K. A wide-area measurement systems-based adaptive strategy for controlled islanding in bulk power systems. *Energies* **2014**, *7*, 2631–2657. [CrossRef]
16. Anaparthi, K.K.; Chaudhuri, B.; Thornhill, N.F.; Pal, B.C. Coherency Identification in Power Systems through Principal Component Analysis. *IEEE Trans. Power Syst.* **2005**, *20*, 1658–1660. [CrossRef]
17. Gomez, O.; Rios, M.A. Real time identification of coherent groups for controlled islanding based on graph theory. *IET Gener. Transm. Distrib.* **2015**, *9*, 748–758. [CrossRef]
18. Avdakovic, S.; Becirovic, E.; Nuhanovic, A.; Kusljugic, M. Generator coherency using the wavelet phase difference approach. *IEEE Trans. Power Syst.* **2014**, *29*, 271–278. [CrossRef]
19. Khalil, A.M.; Iravani, R. A Dynamic Coherency Identification Method Based on Frequency Deviation Signals. *IEEE Trans. Power Syst.* **2016**, *31*, 1779–1787. [CrossRef]

20. Winters-Hilt, S.; Yelundur, A.; McChesney, C.; Landry, M. Support Vector Machine implementations for classification & clustering. *BMC Bioinform.* **2006**, *7*, 1–18.
21. Chow, J.H. *Power System Coherency and Model Reduction*; Springer: New York, NY, USA, 2013.
22. Ben-Hur, A.; Horn, D.; Vapnik, V. Support Vector Clustering. *J. Mach. Learn. Res.* **2001**, *2*, 125–137. [CrossRef]
23. Beamer, S.; Asanović, K.; Patterson, D. Direction-optimizing breadth-first search. *Sci. Program.* **2013**, *21*, 137–148. [CrossRef]
24. Wang, J.S.; Chiang, J.C. A cluster validity measure with outlier detection for support vector clustering. *IEEE Trans. Syst. Man Cybern. Part B (Cybern.)* **2008**, *38*, 78–89. [CrossRef] [PubMed]